

# The lithium abundance in sunspots

S. Ritzenhoff, E.H. Schröter, and W. Schmidt

Kiepenheuer-Institut für Sonnenphysik, Schöneckstr. 6, D-79104 Freiburg, Germany

Received 30 September 1996 / Accepted 21 July 1997

**Abstract.** The solar lithium abundance was determined using an empirical model for an observed sunspot umbra. The atmospheric model is deduced from a number of spectral lines. In addition to the lithium (I) line doublets from  $\text{Li}^6$  and  $\text{Li}^7$  at 670.8 nm eight different line profiles were observed with high spectrographic resolution. A magnetically sensitive line was included in order to determine the magnetic field strength. An estimation for the influence of molecular blends caused by CN and TiO was taken into account.

Under the assumption of LTE a lithium abundance of  $\epsilon_{\text{Li}} = 1.02 \pm 0.12^1$  was derived.

Some evidence for the existence of a small but notable amount of  $\text{Li}^6$  is found, however only an upper limit of  $\text{Li}^6/\text{Li}^7 \leq 0.03$  can be derived. A more precise determination of the isotopic ratio is hampered by the uncertainties induced by the presence of TiO blends.

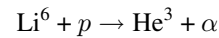
**Key words:** abundances, atmospheres, Sun

## 1. Introduction

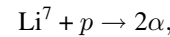
The determination of the lithium abundance is of high importance because of consequences for cosmological models and for the structure and evolution of stars. The primordial lithium is a parameter in big bang models and in the theory of nucleosynthesis of light elements (e.g. Boesgaard & Steigman, 1985). The depletion of the solar lithium of about a factor of a hundred with respect to its original (i.e. meteoritic) abundance (Greenstein & Richardson, 1951) has to be reproduced by models of the solar evolution. The lithium abundance for one solar mass stars depends strongly on the depth of the convection zone and the extra mixing in the overshoot layer (D’Antona & Mazzitelli, 1984).

In the deeper and hotter layers lithium is destroyed by nuclear reactions with protons. Moreover the isotope ratio  $\text{Li}^6/\text{Li}^7$  on the sun differs from the meteoritic one, where  $\text{Li}^6/\text{Li}^7 = 0.08$

(Anders & Grevesse, 1988). This ratio is a sensitive thermometer for the bottom of the convection zone since the isotopes are destroyed at different temperatures. For  $\text{Li}^6$  a temperature of  $\approx 2 \times 10^6$  K is sufficient to produce the reaction:



whereas  $\text{Li}^7$  requires a temperature of  $\approx 2.4 \times 10^6$  K to be destroyed by a proton collision process like



(e.g. Stix, 1991). Model calculations (e.g. Ahrens et al., 1992) predict the total destruction of  $\text{Li}^6$  since in the standard solar model the bottom of the convection zone reaches temperatures of about 2 million degrees and with an overshoot layer of 0.3 pressure scale heights even up to 2.3 million degrees. Therefore  $\text{Li}^6$  and  $\text{Li}^7$  should have been depleted during the pre-main-sequence evolution where the convection zone was even deeper. Since  $\text{Li}^7$  is reduced by a factor of a hundred, virtually no  $\text{Li}^6$  is expected on the main sequence (e.g. Smith et al., 1993).

The  $\text{Li}^6/\text{Li}^7$  isotope ratio is difficult to derive from observational data because the depleted  $\text{Li}^6$  abundance should even in the umbra produce only a very faint line or, confirming the theoretical predictions, give no contribution at all to the  $\text{Li}^7$ -dominated absorption multiplet around 670.8 nm.

Lithium has a low ionization potential of  $\chi_{\text{Li}} = 5.4$  eV, resulting in an equivalent width of the lithium absorption lines formed in the photosphere of the quiet sun of about 0.18 pm (Brault & Müller, 1975). In addition the spectral region around the lithium lines is blended with molecular lines of CN and TiO.

Similarly to what is observed in atmospheres of stars cooler than the Sun the lithium lines are much stronger in sunspots due to the lower degree of ionisation and therefore the influence of blends is smaller.

After the first measurements by Greenstein & Richardson in 1951, who found the lithium abundance ranging between  $\epsilon_{\text{Li}} = 0.7$  and  $\epsilon_{\text{Li}} = 1.6$  the literature gives results ranging from the doubt of the existence of any lithium on the sun (Lynds, 1965) to  $\epsilon_{\text{Li}} = 1.16$  (Steenbock & Holweger, 1984). Table 1 gives an overview of some methods and results for the lithium abundance. After Wiehr et al. (1968) only Engvold et al. (1970) observed sunspot umbrae to derive the lithium

Send offprint requests to: W. Schmidt

<sup>1</sup> On the logarithmic scale, where the abundance of hydrogen is  $\epsilon_{\text{H}} = 12$

**Table 1.** Investigations for the solar lithium abundance: methods and results

1	2	3	4	5	6	7	8	9
Authors	observation	resolution	blends CN/TiO	scattered light	atmospheric model	LTE/ NLTE	$\epsilon_{\text{Li}}$	errors
Greenstein & Richardson (1951)	quiet sun/ penumbra	?	no	no	–	LTE	<b>0.7-1.6</b>	–
Schmahl & Schröter (1965)	sunspot	?	no	yes	–	LTE	<b>0.9</b>	$\pm 0.3$
Wiehr et al. (1968)	sunspot	5 pm	CN<0.5 pm	yes	–	LTE	<b>0.76</b>	$\pm 0.2$
Engvold et al. (1970)	sunspot	1-2 pm	subtracted estimated TiO	yes	Zwaan	LTE	<b>0.80</b>	$\pm 0.25$
Brault & Müller (1975)	quiet sun	?	subtracted estimated CN	no	Holweger, HSRA	LTE, NLTE	<b>1.0</b>	$\pm 0.1$
Steenbock & Holweger (1984)	no obs. results from Müller et al.	–	–	–	Holweger &Müller quiet sun	NLTE	<b>1.16</b>	$\pm 0.10$
This work (1997)	sunspot	<1pm	estimated CN and TiO	no	8 line based semi-empirical	LTE	<b>1.02</b>	$\pm 0.12$

Column 3) is the spectral resolution the authors used, 4) if CN or TiO was taken into account, 5) if a correction for scattered light was made, 6) the atmospheric model that was used to calculate the line profiles, 7) if the results were obtained with an LTE or NLTE model, 8) is the result for the lithium abundance

abundance. They found an anomalous strong line depression (line center  $I_{\text{line}}/I_{\text{cont}} = 0.2$ ). Nevertheless the calculated  $\epsilon_{\text{Li}} = 0.8 \pm 0.25$  was very low.

Brault & Müller (1975) tried to determine the lithium abundance with observations in the quiet sun using different atmospheric models and an approach to NLTE calculations. But in their data set the molecular blends could not be resolved. The estimation of the influence of blends therefore remains doubtful.

Other authors (Grevesse, 1968, Stellmacher & Wiehr, 1971, Steenbock & Holweger, 1984) calculated the lithium abundance on the base of existing data sets. They used different standard models for sunspot umbrae in order to test the model influence on the yielded abundance or calculated it with NLTE radiation transport.

For this work we made new observations of a sunspot to determine the lithium abundance. With our high resolution spectra we could identify molecular blends and reduce the influence of noise better than earlier works. We constructed a multi-line based empirical model of the individual umbra atmosphere to get a good accordance between observed and calculated line profiles.

For the analysis of the lithium abundance the positioning of the spectral continuum is very important. Our model could reproduce the continuum intensity ratio from umbra to quiet sun better than standard models.

Once the atmospheric model was fixed, the lithium abundance was derived from the optimum fit of the computed Li-line profile to the observed one.

## 2. Observations

In August 1994 we made sunspot observations in nine different spectral regions with the 70 cm Vacuum Tower Telescope (VTT) at the Observatorio del Teide, Tenerife. The sunspot with penumbra (NOAA 7762, named "Willy") located at  $\cos \theta = 0.95$  had an umbral diameter of about  $15''$ . A strong lightbridge with nearly photospheric intensity divided the umbra approximately in the ratio of one to two. The seeing conditions for most exposures allowed for a spatial resolution of about  $0.7''$ .

With the echelle-type spectrograph of the VTT three series A to C of three simultaneously observed lines were recorded within 1.5 hours.

We used three large-format CCD cameras with  $1024 \times 1024$  pixels and a pixel size of 19 microns squared. The exposures were taken in the  $2 \times 2$ -binning mode. The spectral resolution for all spectrograms was better than 1 pm.

In addition to the doublets of the lithium resonance lines from the isotopes  $\text{Li}^6$  and  $\text{Li}^7$  at 670.8 nm we selected the magnetically sensitive line Fe I 617.3 nm (Landé factor  $g = 2.5$ ) to determine the magnetic field strength  $B$ , six nonmagnetic ( $g = 0$ ) lines with different atmospheric heights of formation and the K I 769.9 nm line which originates from the same atomic transition as lithium and is similar in most line parameters except the abundance. Table 2 gives an overview of the nine spectral regions and some relevant line parameters.

**Table 2.** Some relevant parameters of the observed lines.

Series	spectral line (nm)	Transition	excitation pot. $\chi$ (eV)	$\log(gf)$
A	Fe I 617.334	$^5P_1 - ^5D_0$	2.22	-3.06
	Li <sup>7</sup> I 670.777	$^2S_{1/2} - ^2P_{3/2}$	0.00	0.00
	Li <sup>7</sup> I 670.793	$^2S_{1/2} - ^2P_{1/2}$	0.00	-0.30
	Li <sup>6</sup> I 670.794	$^2S_{1/2} - ^2P_{3/2}$	0.00	0.00
	Li <sup>6</sup> I 670.809	$^2S_{1/2} - ^2P_{1/2}$	0.00	-0.30
	K I 769.898	$^2S_{1/2} - ^2P_{3/2}$	0.00	-0.14
B	Fe I 406.534	$^5F_1 - ^5D_0$	3.43	-1.38
	Fe I 543.453	$^5F_1 - ^5D_0$	1.01	-2.22
	Fe I 557.610	$^5F_1 - ^5D_0$	3.43	-0.73
C	Fe I 444.320	$^3P_0 - ^3D_1$	2.86	-1.24
	Ni I 491.203	$^5F_1 - ^5F_1$	3.77	-0.87
	Fe I 512.373	$^5F_1 - ^5F_1$	1.01	-3.07

The three lines of each series represent the simultaneously taken sets. For lithium all four components of the line are given. In column 4  $g$  is the oscillator-strength and  $f$  is the statistical weight for the transition.

### 2.1. Data reduction

After standard procedures like dark current subtraction und flat fielding, the instrumental non-dispersed stray light was determined (5%) and subtracted for all spectral regions.

From all spectrograms the average of the ten best exposures was used to extract the photospheric and umbral line profiles. While for the quiet sun a spatial area of about 10 arcsec could be averaged, the umbra profiles were extracted out of a smaller area ( $\approx 1$  arcsec) in the darkest region of the spot. Instead of using a spatially fixed region we selected the darkest part of the umbra that was imaged onto the entrance slit of the spectrograph. Hence we avoided large variations of the umbral temperature or the influence of umbral dots appearing randomly on the slit through image motion.

An example of a slitjaw image is given in Fig. 1.

Since the atmospheric component of scattered light was not determined empirically it was taken into account in the numerical calculations. To reproduce the amount of scattered light, the calculated model had to reproduce the observed intensity ratio of the continuum level in umbra and photosphere.

With the photospheric reference model VAL-C (Vernazza et al., 1981) radiative transport calculations were made to test the required atomic parameters. Tabulated  $\log(gf)$  values were taken from Thévenin (Thévenin, 1989) and verified or adjusted by a comparison between computed line profiles and ones from a spectral Atlas (Delbouille et al., 1973). The so found parameters were later used as input data for the calculations of the new umbra model.

### 2.2. Magnetic field strength $B$

As the lithium resonance lines are Zeeman-sensitive with Landé factors of  $g_{\text{eff}} = 1.33$  and  $g_{\text{eff}} = 1.167$  respectively, it was necessary to get information on the magnetic field strength of the spot. The Fe I 617.3 nm line with a Landé factor of  $g = 2.5$

and a splitting scheme of a Zeeman triplet (Beckers, 1969) was used to determine the field strength. For of a simple triplet one obtains the field strength by measuring the splitting between  $\pi$ - and  $\sigma$ -components and using the Zeeman equation:

$$\Delta\lambda_B = 4.67 \times 10^{-12} g_{\text{eff}} \lambda_0^2 |B|,$$

that specifies the relationship between the wavelength shift of the  $\sigma$ -components  $\Delta\lambda_B$  relative to the wavelength of the unshifted line position  $\lambda_0$  ( $\pi$ -component) given in nanometer and the magnetic field strength  $|B|$  in Gauß.

The field strength was found to  $B = 2450$  Gauß in an optical height of  $\log \tau_{500} = -2.5$ .

To obtain the field strength in a range of height that includes all components of the lithium line a gradient of the magnetic field of 2 Gauß/km was assumed, adopting empirical results from Balthasar & Schmidt (1993).

The angle between surface normal and the line of sight was  $\theta = 20^\circ$ . We tested inclination angles of the magnetic field lines between  $\gamma = 0^\circ$  and  $\gamma = 30^\circ$  in order to check their influence on the computed line profiles. We got the best results with an inclination angle of  $\gamma = 20^\circ$  as expected.

## 3. The empirical umbra model

The empirical model for the umbra atmosphere of our sunspot was determined in three steps:

- Comparison of the observed continuum intensity ratios of umbra to photosphere with computed ratios obtained from a reference photosphere and umbra model atmospheres of different effective temperatures.
- Interpolation between a hotter and a cooler umbra model to reproduce observed continuum intensity ratios.
- Fit of the computed line profiles of all observed lines representing different layers of formation to observed ones by fine adjustment of the model atmosphere step by step for all heights. In every iteration a complete atmospheric model with temperature, gas pressure and electron pressure stratification was calculated under the assumption of hydrostatic equilibrium.

### 3.1. The continuum intensity ratio

The continuum intensity ratio of umbra to photosphere  $I_{\text{umbra}}^{\text{cont}}/I_{\text{phot}}^{\text{cont}}$  with the models M4 (Kollatschny et al., 1980) and IAC-hot (Collados et al., 1994) for the umbra and the VAL-C model for the photosphere were used to reproduce the observed continuum contrasts as a function of wavelength.

It turned out that the M4 was a lower and the IAC-hot model was an upper temperature limit for the observed sunspot. Starting from the M4 model we corrected to higher temperatures that led to higher emission intensities using the Stefan-Boltzmann law ( $I \propto \sigma T^4$ ).

This model was finetuned in order to obtain a good fit to the observed line profiles. Figure 2 shows the continuum contrast as a function of wavelength as obtained with the final model.

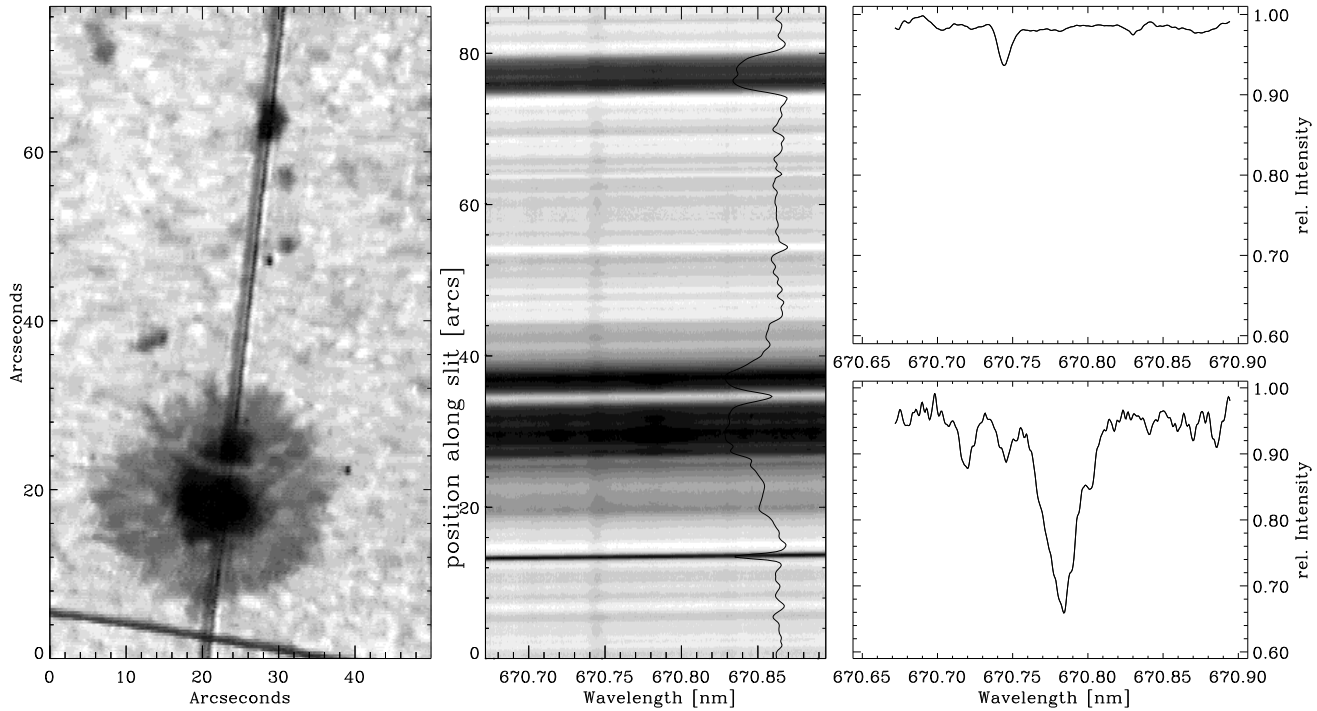


**Fig. 1.** Left: White light slitjaw image of sunspot "Willy" in poor video registration quality. Middle: Spectrum at 670.8 nm with vertically plotted intensity profile. Right: Extracted line profiles of lithium. The upper figure shows the averaged quiet photospheric profile, the lower one the profile in the sunspot umbra. The intensity range for both profiles is the same to demonstrate the large increase of lithium absorption in the umbra.

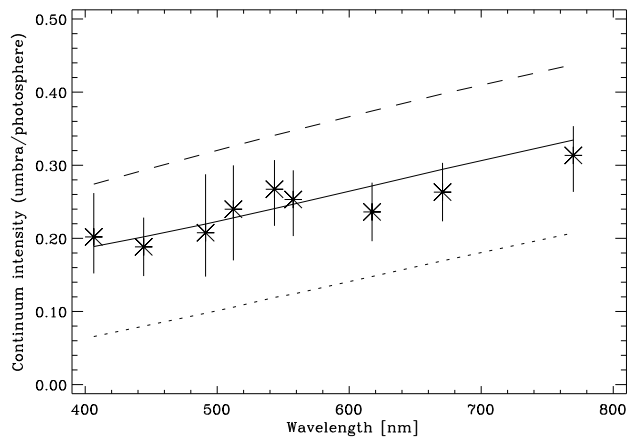


**Fig. 2.** The continuum intensity ratio of umbra to photosphere as a function of wavelength. The stars represent the observations. The error bars result from the range of all exposures. The quiet photosphere intensity was computed with VAL-C. The dotted and dashed lines show the calculated intensity ratio using M4 and IAC-hot for the umbra respectively. The full line represents the result obtained with our model.

### 3.2. The temperature stratification

The temperature stratification is the most important parameter of the umbra model atmosphere, since the lithium resonance

lines are very sensitive to absolute temperature and temperature gradient.

In an iterative procedure we computed line profiles with the preliminary model and compared them to our observations. The code we used for the radiative transport calculations (Grossmann-Doerth, 1988) starts from an optical depth of  $\log \tau_{500} = 2$  and takes into account all contributions up to  $\log \tau_{500} = -5$ .

Due to the different heights of formation of our spectral lines the temperature of the model atmosphere could be adopted over a wide range of heights. Step by step radiative transport calculations from the lower to the higher formed lines were made to fit all synthetic lines to the observed ones.

Figure 4 shows the resulting temperature versus the optical depth of the new umbra atmosphere that allowed to reproduce all line profiles but the highest ones correctly. The other models are plotted to emphasize that the temperature stratification from our analysis is between the relatively hot model from Collados et al. and the cooler M4 model.

A comparison between observed and calculated line profiles is given in Fig. 3.

Table 3 shows the formation heights for the photospheric line cores including both lithium doublets. It should be noted that some of these lines are formed over a wide range of heights. The Fe I 543.4, Fe I 512.3 and K I 769.9 nm lines have so much contribution from high layers, that the weighted center is

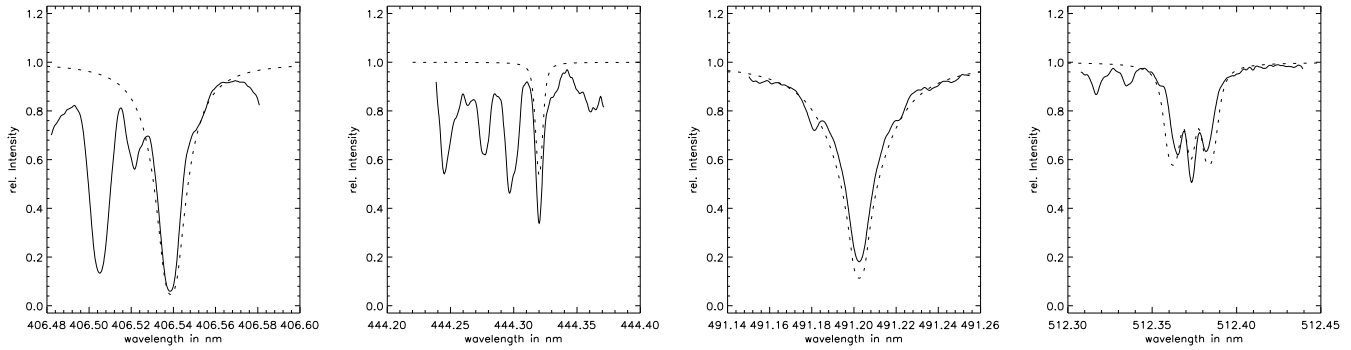


**Fig. 3.** Synthetic line profiles (dotted) calculated with our umbra model in comparison to observed profiles.

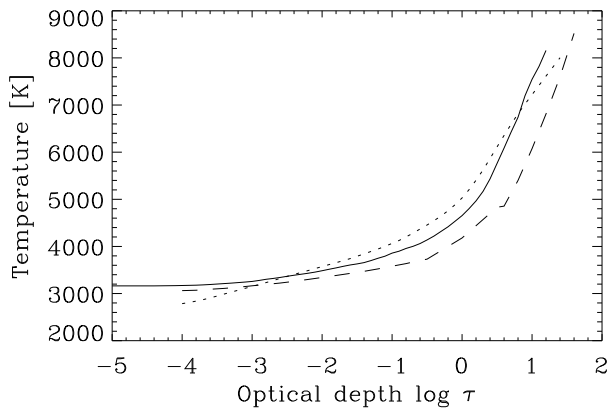


**Fig. 4.** Temperature versus optical depth ( $\log \tau_{500}$ ) of our empirical umbra model (solid) in comparison to the model M4 (dashed) and the IAC-hot model (dotted).

**Table 3.** Weighted formation heights of line cores in the umbra

Test lines [nm]	$\log \tau_{500}$	lithium lines [nm]	$\log \tau_{500}$
Ni I 491.2	-0.9	$Li^7$ 670.777	-2.65
Fe I 406.5	-2.1	$Li^7$ 670.793	-2.5
Fe I 617.3	-2.5	$Li^6$ 670.794	-2.5
Fe I 557.6	-3.2	$Li^6$ 670.809	-2.45
Fe I 444.3	-3.4		

above  $\log \tau_{500} = -5$  and have therefore omitted from further analysis.

### 3.3. The blends in the lithium line

The determination of the lithium abundance is complicated by the occurrence of blends of molecular lines from TiO and CN. Engvold et al. (1970) and Brault & Müller (1975) have searched in vain for further blends, e.g. terrestrial lines around 670.8 nm, so that other contributions to the absorption of lithium can be excluded. In Fig. 5 we indicate the location of molecular blends from TiO (Phillips, 1951) and CN (Davis & Phillips, 1963) rotational absorption bands. The influence of molecular blends in the umbral spectrum is estimated to be much weaker than in the quiet photosphere (Engvold et al., 1970), where effects on

the lithium lines with an equivalent width of about 0.18 pm are extremely difficult to determine. The computed equivalent width of the two lithium doublets of 9.4 pm is slightly smaller than the observed one of 10.3 pm. From this difference we derived an upper limit for the contribution of blends on the whole absorption feature:

$$W_{\text{CN,TiO}}/W_{\text{Li+(CN,TiO)}} \leq 0.09$$

## 4. The lithium abundance

Using the new umbra model atmosphere that could reproduce all line profiles except those which are formed in the highest, nearly chromospheric layers, we computed the lithium lines with the abundance as the only free parameter.

In a first run we assumed a pure  $Li^7$  composition with no contributions of  $Li^6$ . In steps of 0.03 dex, the smallest discernable change in equivalent width and line profile, we computed profiles with abundances ranging from  $\epsilon_{Li} = 0.79$  to  $\epsilon_{Li} = 1.24$ .

The best fit for a pure  $Li^7$  absorption was achieved for a lithium abundance of  $\epsilon_{Li^7} = 1.00$ . A slightly stronger absorption in the observed profile was admitted at the locations of the molecular blends.

### 4.1. The isotope-ratio $Li^6/Li^7$

Ahrens et al. (1992) predict the total destruction of  $Li^6$  on the solar surface due to the mixing at the bottom of the convection zone with material hotter than 2 million degrees.

From observations one can derive an upper limit for the ratio  $Li^6/Li^7$ , but cannot confirm the absence of any  $Li^6$ . This uncertainty is mainly due to the unknown strength of the TiO blends (see also Sect. 5).

We added for every step of the  $Li^7$  abundance between zero and three percent of  $Li^6$  to fit the observed line profile. The accordance between calculated and observed line profiles was better with a small but notable amount of  $Li^6$  even when contributions of the TiO blends at 670.792 and 670.816 nm were taken into account. Figure 5 shows the best fit of the computed to the observed line profile. It corresponds to a value for the  $Li^7$  abundance of  $\epsilon_{Li^7} = 1.00$  plus a small amount of  $\epsilon_{Li^6} = 0.02$ .

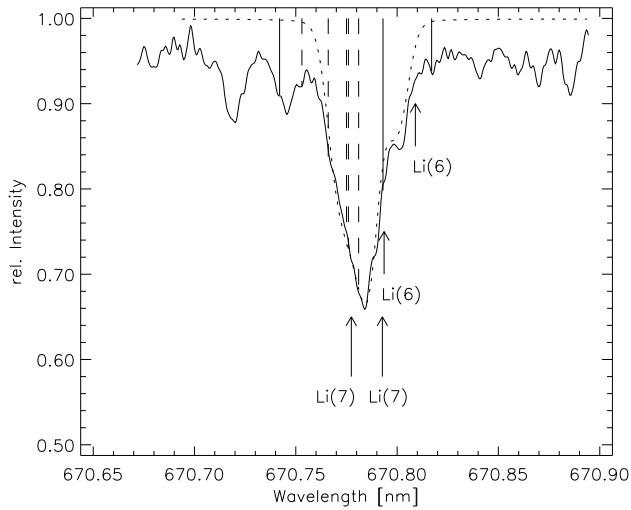


**Fig. 5.** Best accordance of the observed lithium line profile and the synthetic one computed with the new individual atmosphere. In this case the total lithium abundance is  $\epsilon_{\text{Li}} = 1.02$  and the ratio  $\text{Li}^6/\text{Li}^7 = 0.02$ . The location of the molecular blends of CN (dashed) and TiO (solid) are also given.

Hence, the total lithium abundance results to:

$$\epsilon_{\text{Li}^6 + \text{Li}^7} = 1.02$$

We estimate the total error to be lower than 0.12 dex in the abundance of lithium. The error represents mainly the uncertainty of the atmospheric model as the most important influence on the result (in accordance with Stellmacher & Wiehr, 1971). The uncertainty in the positioning of the continuum gives an error in the range of 0.05 dex. Other uncertainties are due to the step-width in the calculations (0.03 dex) and in the estimation of the molecular blends (0.03 dex).

## 5. Discussion and conclusions

Sunspot observations in nine spectral regions were made in order to determine the lithium abundance with an atmospheric model derived for the observed umbra. Three series of three simultaneously observed lines made it possible to construct a consistent umbral model.

The observed spectra have high spectral resolution ( $\lambda/\delta\lambda \approx 800000$ ) and cover with their heights of formation a wide range of optical depth ( $\log \tau_{500} \approx -0.9 \dots 3.7$ ).

Because of the high spectral resolution some of the TiO and CN molecular blends could be identified and their influence on the lithium profile estimated with an uncertainty of about three percent or 0.03 dex. Hence the molecular blends are of lower importance for the lithium abundance derived from sunspot spectra, in good accordance with earlier results (Engvold et al., 1970).

For the isotope ratio an upper limit of  $\text{Li}^6/\text{Li}^7 \leq 0.03$  could be found. This limit is obtained, when the absence of blends is assumed and the computed line depression in the red wing reaches the observed one. However, there is some evidence for the existence of  $\text{Li}^6$  on the solar surface because the red wing

of the line can't be explained solely by TiO blends (see Fig.5). From the best fit of the synthetic to the observed line profile we derive a value of 0.02 for the ratio  $\text{Li}^6/\text{Li}^7$ . A more conclusive statement for this evidence with a quantitative result could only be made with a precise knowledge of the strength of the two TiO blends at 670.792 and 670.816 nm.

### 5.1. Sources for systematic errors

One sensitive factor to get a correct absorption profile of lithium is the determination and subtraction of atmospheric stray light. Unfortunately no additional observations to investigate the dispersed scattered light were made for this work, so that this uncertainty had to be accepted as an additional free parameter in the deduction of the model atmosphere. Although the model was able to reproduce the ratio of the umbra continuum intensity to the photospheric one there remains some uncertainty in the real umbra continuum level that might lead to a slightly lower or higher absolute absorption. The corresponding variation of the lithium abundance is  $\leq 0.05$  dex.

The influence of the atmospheric model is of high importance. Assuming a straylight of about 5% the intensity ratios should shift towards the M4 model (see Fig.2). However the M4 model has a much too low effective temperature for our relatively small spot. The comparison of calculated and observed lines together with the reproduced continuum intensity ratios shows that the adopted model is a rather good approximation.

### 5.2. NLTE effects

All calculations were made under the assumption of local thermodynamic equilibrium (LTE). Non-LTE effects should be taken into account because parts of the lithium lines are formed in higher, even chromospheric layers. Lower temperature and hydrostatic pressure in the umbra atmosphere, lower collision rates because of lower density and temperature and the small lithium abundance might lead to non-LTE effects. A deviation from LTE for lithium is predicted for atmospheres of cooler stars in a recent work by Carlsson et al. (1994).

The present data set does not allow an adequate quantitative analysis of the non-LTE influence on the lithium abundance (H.J.M.J. Bruls, private communication).

For our future investigations we want to construct an individual umbra atmosphere with a larger and different data set that allows to determine the temperature stratification consistently with the NLTE treatment of the lithium line.

A precise measurement of the rotational bands of the TiO and CN lines would allow for a better determination of the  $\text{Li}^6/\text{Li}^7$  isotope ratio.

*Acknowledgements.* The authors wish to thank Michael Knölker for valuable discussions and his critical reading of the manuscript. We also wish to thank the referee for his detailed and fruitful comments.

## References

- Anders E., Grevesse N., 1988, *Geochimica et Cosmochimica Acta* 53, 197

- Ahrens B., Stix M., Thorn M., 1992, A&A 264, 673  
Balthasar H., Schmidt W., 1993, A&A 279, 243  
Beckers J.M., 1969, A Table of Zeeman Multiplets, AFCRL Phys. Science research papers  
Boesgaard A.M., Steigmann G., 1985, ARA&A 23, 319  
Brault J.W., Müller E.A., 1975, SP 41, 43  
Carlsson M., Rutten R.J., Bruls H.J.M.J., Shchukina N.G., 1994, A&A 288, 860  
Collados M., Martinez-Pillet V., Ruiz-Cobo B., del Toro Iniesta J.C., Vazquez M., 1994, A&A 270, 494  
D'Antona F., Mazzitelli I., 1984, A&A 138, 431  
Davis S.P., Phillips I.G., 1963, *The Red System  $A^2\Pi - x^2\Sigma$  of the CN molecule*, University of California Press, Berkeley  
Delbouille L., Neven L., Roland G., 1973, *Photometric atlas of the solar spectrum from 3000 Å to 10000 Å*, Institut d'Astrophysique de l'Université de Liège  
Engvold O., Kjeldseth Moe O., Maltby P., 1970, A&A 9, 79  
Greenstein I.L., Richardson R.S., 1951, ApJ 113, 536  
Grevesse N., 1968, SP 5, 159  
Grossmann-Doerth U., Larson B., Solanki S.K., 1988, A&A 204, 266  
Kollatschny W., Stellmacher G., Wiehr E., Falipou M.A., 1980, A&A 86, 245  
Lynds C.R., 1965, ApJ 142, 396  
Phillips I.G., 1951, ApJ 111, 314  
Schmahl G., Schröter E.H., 1965, Z. Astrophys. 62, 143  
Smith V.V., Lambert D.L., Nissen, P.E., 1993, ApJ 408, 262  
Stellmacher G., Wiehr E., 1971, SP 21, 96  
Stellmacher G., Wiehr E., 1988, A&A 191, 149  
Steenbock W., Holweger H., 1984, A&A 130, 319  
Stix M., 1991, *The Sun*, Springer, Berlin Heidelberg  
Thévenin F., 1989, A&A Suppl. Ser. 77, 137  
Vernazza J.E., Avrett E.H., Loeser R., 1981, ApJS 45, 635  
Wiehr E., Stellmacher G., Schröter E.H., 1968, Astrophysical Letters 1, 181